

See discussions, stats, and author profiles for this publication at: <https://www.researchgate.net/publication/5755841>

Ab Initio Comprehensive Conformational Analysis of 2'-Deoxyuridine, the Biologically Significant DNA Minor Nucleoside, and Reconstruction of Its Low-Temperature Matrix Infrared Spe...

ARTICLE in THE JOURNAL OF PHYSICAL CHEMISTRY B · JANUARY 2008

Impact Factor: 3.3 · DOI: 10.1021/jp074747o · Source: PubMed

CITATIONS

44

READS

24

5 AUTHORS, INCLUDING:



Yevgen Yurenko

Masaryk University

27 PUBLICATIONS 455 CITATIONS

SEE PROFILE



Mahmoud Ghomi

Université Paris 13 Nord

112 PUBLICATIONS 1,777 CITATIONS

SEE PROFILE



Dmytro Mykolayovych Hovorun

National Academy of Sciences of Ukraine

391 PUBLICATIONS 2,057 CITATIONS

SEE PROFILE

Ab Initio Comprehensive Conformational Analysis of 2'-Deoxyuridine, the Biologically Significant DNA Minor Nucleoside, and Reconstruction of Its Low-Temperature Matrix Infrared Spectrum

Yevgen P. Yurenko,^{†,‡,§} Roman O. Zhurakivsky,[‡] Mahmoud Ghomi,^{‡,§}
Svitlana P. Samijlenko,[†] and Dmytro M. Hovorun^{*,†}

Department of Molecular and Quantum Biophysics, Institute of Molecular Biology and Genetics, National Academy of Sciences of Ukraine, vul. Zabolotnoho 150, 03143, Kyiv, Ukraine, UMR CNRS 7033, Laboratoire de Biophysique Moléculaire, Cellulaire et Tissulaire (BioMoCeTi), Université Pierre et Marie Curie, GENOPOLE-Campus 1, 5 rue Henri Desbrières, 91030 Evry Cedex, France, UFR SMBH, Université Paris 13, 74 rue Marcel Cachin, 93017 Bobigny cedex, France, and Department of Quantum Radiophysics, Faculty of Radiophysics, Taras Shevchenko Kyiv National University, pr. Hlushkova 2, korp. 5, 03127, Kyiv, Ukraine

Received: June 19, 2007; In Final Form: September 21, 2007

A comprehensive conformational analysis of isolated 2'-deoxyuridine (dU), a minor DNA nucleoside, has been performed by means of ab initio calculations at the MP2/6-311++G (d,p)//DFT B3LYP/6-31G (d,p) level of theory. At 298.15 and 420 K, all 94 allowed conformers of dU are within 8.96 and 7.91 kcal/mol Gibbs energy ranges, respectively. Syn orientation for the base and South (S) conformers for the sugar dominate at 298.15 K: syn/anti = 62.3%:37.7% and S/N = 77.2%:22.8%. At 420 K in the majority of conformers, the base is anti oriented and the population of North (N) sugars increases: syn/anti = 39.3%:60.7% and S/N = 63.0%:37.0%. Values of all conformational parameters and correlations between them, as well as their correlations with valence bonds, and also correlations between valence bonds and angles were estimated. In general, 14 types of intramolecular H-bonds were detected (1–3 H-bonds per conformer, the total number 175), namely, C1'H...O2 (16 H-bonds), C2'H1...O5' (9), C2'H2...O2 (21), C3'H...O2 (21), C5'H1...O2 (14), C5'H2...O2 (11), C6H...O4' (37), C6H...O5' (22), C3'H...HC6 (4), O5'H...HC6 (2), O3'H...O5' (5), O5'H...O4' (1), O5'H...O3' (4), and O5'H...O2 (8). Geometric, vibrational, structural-topological, and energetic features of the OH...O intramolecular H-bonds in dU conformers were determined. The close similarity between energetic and geometric characteristics of dU and thymidine DNA-like conformers in anti and relevant syn conformations and their transition states of the anti → syn interconversion implies that mismatch DNA glycosylase discriminates between the two nucleosides, mainly because of the difference in the shapes of their bases. Convolution of calculated IR spectra of all the dU conformers within the limits 3400–3700 cm⁻¹ appears to be consistent with its low-temperature matrix IR spectrum (Ivanov et al. *Spectrochim. Acta, Part A* **2003**, 59, 1959), wavenumber discrepancy not exceeding 1%. It was concluded that, for a reliable reproduction of the experimental spectrum, the whole set of conformers should be taken into consideration. The suggested method makes reconstruction of the isolated nucleoside IR spectrum at a physiological interval of temperature reasonably possible.

I. Introduction

Conformational analysis of canonical nucleosides is an important problem of structural biology, molecular biophysics, biochemistry and pharmacology.¹ The investigation of the structural, dynamical, and physicochemical properties of nucleosides plays a key role in a deeper understanding of nucleic acids' structure and functioning. Information about the conformational properties of nucleosides in crystal phase has been obtained by X-ray analysis.^{2–5} Data on conformational behavior of nucleosides can be derived from infrared^{6,7} and Raman⁸ spectroscopy as well as from neutron inelastic scattering at low temperatures.^{9,10}

By NMR spectroscopy, the most extensive information about nucleosides' spatial structure and conformational transition barriers can be obtained from their solutions (aqueous, non-aqueous, and mixed).^{11–14} Acoustic spectroscopy proved to be helpful in the study of changes of a base orientation against deoxyribose moiety.^{15,16} The sugar residue role in the interactions of nucleosides with amino acids' carboxylic group was elucidated in model systems of protein–nucleic acids' recognition by ¹H NMR spectroscopy.^{17,18} Unique data on nucleosides' intrinsic conformational properties in the gas phase¹⁹ and in low-temperature matrices^{20,21} came from Fourier transform infrared and double resonance spectroscopic experiments. Ab initio calculations^{22–32} substantively complement our knowledge of nucleosides, but those works deal only with some selected conformers.

The present paper is devoted to a comprehensive conformational analysis of isolated 2'-β-deoxyuridine (dU), a biologically

* To whom correspondence should be addressed. Phone: +38-044-526-11-09. Fax: +38-044-526-07-59. E-mail: dhovorun@imbg.org.ua.

[†] National Academy of Sciences of Ukraine.

[‡] Université Pierre et Marie Curie.

[§] Université Paris 13.

[‡] Taras Shevchenko Kyiv National University.

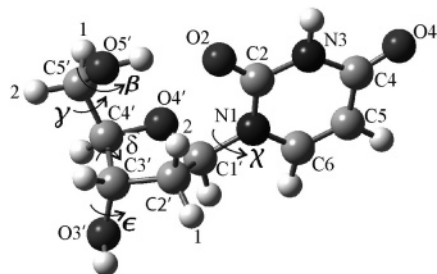


Figure 1. Atom numbering and nomenclature of dihedral angles of dU. Figure shown is relative to the lowest energy conformer (Conformer 1, see Table 1).

significant DNA minor nucleoside. To our knowledge, in literature there are no exhaustive data on its conformational characteristics. A small amount of the RNA canonical base uracil may be present in DNA due to cytosine deamination or the 2'-β-deoxyuridine monophosphate (dUMP) misincorporation during replication.³³ If not repaired after DNA replication, deamination of cytosine to uracil is one of promutagenic events leading to the G:C → G:T transition mutation.³⁴ The U:A mispairing in DNA results in a less harmful, but cytotoxic, lesion. In normally functioning cells, special enzymes, called DNA glycosylases, prevent such lesion accumulation.³⁵ In human tumor cells, a higher amount of dU frequently occurs.

Deamination of cytosine in DNA may be spontaneous (70–200 events in a cell per day) or caused by the detrimental action of γ radiation and drug treatment.³⁶ However, in B-cell (B-lymphocyte) uracil in DNA, resulting from the cytosine deamination by activation-induced deaminase, is also a physiological intermediate in acquired immunity as a tool for the antibody diversification process.^{36,37} Thus, dU, being a source of malignancy and, at the same time, playing a key role in the adaptivity of the immune system, deserves thorough and comprehensive investigations of its physical and chemical properties.

II. Calculation methods

Chemical structure, atom numbering and dihedral angles' indications are presented in Figure 1. The methodology of conformational analysis was described earlier.³⁸ At first we determined a complete family of conformers for 1', 2'-dideoxyribose (a model sugar residue for 2'-deoxyribonucleosides), which appeared to be 56 in number.³⁹ In search of all the possible dU conformers, we formed up to 10 starting conformations of the nucleoside (proceeding from each conformation of sugar residue), which differ solely in the angle χ value (initial values of angles χ were chosen in such a way that they would cover ranges $90^\circ \geq \chi_{\text{syn}} \geq 0^\circ$ and $270^\circ \geq \chi_{\text{anti}} \geq 180^\circ$ as evenly as possible), and then optimized them without any constraints. Completeness of the obtained family of dU conformers was assured by the absence of new conformers upon almost doubling the number of the nucleoside starting conformations, corresponding to each conformation of sugar residue.

Density functional theory (DFT) calculations using Becke's three-parameter exchange functional⁴⁰ and the gradient-corrected functional of Parr and Yang,⁴¹ and Lee et al.⁴² were used in dU conformational analysis. All the energy optimizations and subsequent harmonic vibrational calculations were performed applying the 6-31G(d,p) standard basis set. The absence of imaginary frequencies proved the calculated conformers to be local minima on the free Gibbs energy (ΔG) landscape. Calculations of vibrational spectra were also used for estimation of Gibbs energies at 298.15 K and 420 K (temperature of the nucleoside evaporation in the low-temperature matrix isolation

experiment) and for reconstruction of IR spectrum of dU isolated in argon matrix.²⁰ To consider electron correlation effects more precisely, for all conformers, single point calculations were performed by the Møller–Plesset second-order perturbation method (MP2) with a larger set of Gaussian basis functions 6-311++G(d,p). The ΔG values were sums of electron energies calculated at the MP2/6-311++G(d,p) level, and the zero-point energies, thermal corrections, and entropy contributions were calculated at the B3LYP/6-31G(d,p) level of theory.

The anti → syn transition states for DNA-like conformers^{23,24} of dU and thymidine (T) were determined by a synchronous transit-guided quasi-Newton method (STQN).⁴³ All the calculations were carried out using the Gaussian 03⁴⁴ program package running on IBM SP3 workstations. The conformational flexibility of dU (such structural parameters as lengths of valence bonds and values of valence angles) was described by a value Δ, which is equal to a structural parameter standard deviation divided to its mean value. In these cases, when both or one conformational characteristic, studied for correlation between them, changes circularly from 0° to 360° to calculate coefficients of correlation, we applied the method⁴⁵ developed for nucleosides in the crystal state. In all other cases, coefficients of correlation were calculated with the standard formulas.⁴⁶

The atoms in molecules (AIM) electron density topology approach⁴⁷ was applied to all the allowed conformers in order to identify intramolecular H-bond stabilizing conformers, according to criteria proposed by Koch and Popelier.⁴⁸ The presence of a bond critical point (BCP, the so-called (3,−1) point) and a bond path between hydrogen donor and acceptor as well as a positive value of Laplacian of the density at BCP were considered as necessary conditions for H-bond formation. The AIMAC⁴⁹ package was used for identification of H-bonds. Wave functions for AIM analysis were calculated at the DFT B3LYP/6-31G(d,p) level of theory. Furthermore, H-bonds were tested on the basis of vibrational and geometric criteria.

The strengths of intramolecular hydrogen bonds OH...O were also evaluated by Grabowski complex measure^{50,51} based on the geometrical and topological parameters of the X–H (here X=O) valence bond:

$$\Delta_{\text{com}} = \{[(r_{\text{X-H}} - r_{\text{X-H}}^0)/r_{\text{X-H}}^0]^2 + [(\rho_{\text{X-H}}^0 - \rho_{\text{X-H}})/\rho_{\text{X-H}}^0]^2 + [(\nabla^2 \rho_{\text{X-H}} - \nabla^2 \rho_{\text{X-H}}^0)/\nabla^2 \rho_{\text{X-H}}^0]^2\}^{1/2} \quad (1)$$

where $r_{\text{X-H}}$, $\rho_{\text{X-H}}$, and $\nabla^2 \rho_{\text{X-H}}$ correspond to the parameters of a proton donating the valence bond involved in H-bonding (valence bond length, electron density at the H–X valence BCP, and the Laplacian of electron density, respectively), and $r_{\text{X-H}}^0$, $\rho_{\text{X-H}}^0$, and $\nabla^2 \rho_{\text{X-H}}^0$ correspond to the same parameters of the X–H valence bond not involved in H-bonding. H-bond energies were evaluated by the empirical Iogansen's formula:⁵²

$$-\Delta H = 0.33(\Delta\nu - 40)^{1/2} \quad (2)$$

where $-\Delta H$ is the H-bond energy in kcal/mol and $\Delta\nu$ is the frequency shift of an H-bonded stretching mode, $\nu(\text{OH})$ (in cm^{-1}). The shifts of stretching modes were calculated as differences between the average frequencies of all conformers without relevant H-bond and the frequencies upon H-bonding. The B3LYP/6-31G(d,p)-calculated frequencies were scaled with a scaling factor equal to 0.9485, chosen in such a way that the conformationally insensitive frequency of the N3H bond stretching vibration, $\nu(\text{N3H})$, would be the same in the experimental²⁰ and calculated spectra. The contribution of each conformer to the intensity of bands in the calculated spectrum, as well as to

conformational equilibrium, was evaluated using the Boltzmann factor $\exp(-\Delta G/kT)$, where ΔG is the relative Gibbs energy.

III. Results and Discussion

Energetic and Geometrical Data. The 94 conformers of the isolated dU molecule were found within the Gibbs energy ranges $\Delta G = 0$ –8.96 kcal/mol at 298.15 K and $\Delta G = 0$ –7.91 kcal/mol at 420 K (Table 1, Figure 2). The completeness of the dU conformational family obtained enables unambiguous identification of the most energetically favorable conformers at both temperatures. The 1.82–8.17 D dipole moment range provides evidence of the variable polarity of the nucleoside conformers (Table 1). An overall examination of the six torsion angles, defining the conformational space of the nucleoside, leads us to conclude the following: (i) The glycosidic angle, χ , defining the relative orientation of the base against the sugar, presents a bimodal distribution (Figure 3), ranging in the following domains: $-171.5^\circ \leq \chi_{\text{anti}} \leq -114.6^\circ$ (53 conformers) and $56.9^\circ \leq \chi_{\text{syn}} \leq 82.0^\circ$ (41 conformers). Since anti conformers prevail in number over syn ones and cover a wider range of χ values, they may be considered as being less restricted by noncovalent interactions between the base and the sugar residue. (ii) In contrast, a trimodal distribution was obtained for the γ , β , and ϵ angles (Figure 3), i.e., $42.8^\circ \leq \gamma_{\text{g}+} \leq 65.0^\circ$ (31 conformers), $158.9^\circ \leq \gamma_{\text{t}} \leq 190.4^\circ / -169.6^\circ$ (34 conformers), and $-75.2^\circ \leq \gamma_{\text{g}-} \leq -54.3^\circ$ (29 conformers); $39.9^\circ \leq \beta_{\text{g}+} \leq 88.3^\circ$ (33 conformers), $167.7^\circ \leq \beta_{\text{t}} \leq 193.4^\circ / -166.6^\circ$ (30 conformers), and $-85.4^\circ \leq \beta_{\text{g}-} \leq -31.1^\circ$ (31 conformers); $32.8^\circ \leq \epsilon_{\text{g}+} \leq 68.4^\circ$ (33 conformers), $172.0^\circ \leq \epsilon_{\text{t}} \leq 209.0^\circ / -151.0^\circ$ (31 conformers), and $-101.5^\circ \leq \epsilon_{\text{g}-} \leq -55.5^\circ$ (30 conformers). (iii) The torsion angle, δ , on which the sugar conformation depends, manifests the distribution divided into two sectors according to North (N) and South (S) conformers (Figure 3), i.e., $73.7^\circ \leq \delta_{\text{N}} \leq 100.0^\circ$ (46 conformers) and $126.6^\circ \leq \delta_{\text{S}} \leq 157.6^\circ$ (48 conformers). Sugar conformation is generally defined by the phase angle of pseudorotation, P ,⁵³ with a bimodal distribution, as discussed above the δ angle (Figure 3), $6.6^\circ \leq P_{\text{N}} \leq 48.7^\circ$ (46 conformers) and $137.9^\circ \leq P_{\text{S}} \leq 215.0^\circ$ (48 conformers). At that, some S and N conformers are beyond the corresponding classical C2'-endo and C3'-endo subfamilies. The C2'-endo and C3'-endo subfamilies are the most densely populated (33 and 40 conformers, respectively). Populations of other subfamilies are the following: the C3'-exo (S) subfamily includes 13 conformers, the C4'-exo (N) subfamily includes 6 conformers, and the C1'-exo (S) subfamily includes 2 conformers. The P angle covers a wider range of variation for S conformers, as well as the sugar pucker amplitude ν_{max} (Figure 2). The algebraic sum of dihedral angles ν_i ($i = 0, 1, \dots, 4$)¹ is close to 0 for all conformers and falls into the -1.0° to 1.2° range; its average equals 0.2° .

Furthermore, it was established that the base residue undergoes subtle perturbations upon the nucleoside formation. In all the conformers, the base heterocycle appeared to be nonplanar, unlike the free base.⁵⁴ Among six torsional angles describing the base nonplanarity, C6N1C2N3, C5C6N1C2, N1C2N3C4, C4C5C6N1, N3C4C5C6, and C2N3C4C5, the first three are the most dependent on the nucleoside formation; i.e., they fall into the largest ranges of values: -3.7° to 4.9° , -4.5° to 3.5° , and -2.7° to 2.7° , respectively. The other three angles cover rather narrower ranges: -1.4° to 1.3° , -1.2° to 0.4° , and -0.5° to 0.9° , accordingly. These six concerned angles correlate with each other in such a way that their algebraic sum is closed to 0, and its absolute value does not exceed 0.2° .

An interesting structural feature is the glycoside bond C1'N1 deviation from the base mean plane (a mean plane was defined

so as to minimize the sum of the base atoms squared distances from it). The angle between the C1'N1 bond and the base mean plane falls into the range from -3.6° to $+6.9^\circ$ (the “+” means the right-handedness of the three vectors N1C2, N1C6, and N1C1'). The torsional angles C1'N1C6C5 and C1'N1C2N3 vary within the -172.6° to -176.6° and -176.2° to -172.6° limits, respectively. It was not clear whether the base nonplanarity and the glycoside bond deviation from the base plane, observed in the crystal-state X-ray studies for pyrimidine nucleosides,^{1,5} are determined only by crystal packing forces or intramolecular interactions contribute as well. Comparison of our results with crystallographic data⁵ (Table 2) clearly demonstrates both intramolecular and intermolecular contributions to the effect. Interestingly, dU forms typically heteromolecular crystal,⁴ which consists of two slightly different molecules **M1** and **M2** corresponding to conformer **28** of the isolated nucleoside with $\Delta G = 2.40$ kcal/mol (Tables 1, 2).

Additionally, the N1C1' glycosylic bond (mean length 1.478 Å) is the most conformationally dependent; it covers the 1.458–1.499 Å range, and its Δ parameter is equal to 0.007. Values of the Δ parameter for valence bonds in the base residue are the following: for the N1C2 bond, the Δ parameter amounts to 0.003; for N1C6 and C2O2 bonds, it is equal to 0.002; the 0.001 value corresponds to the C2N3, N3C4, C4C5, C4O4, C5C6, and C6H bonds. The N3H and C5H bonds are not conformationally dependent ($\Delta < 0.0005$). In general, the sugar valence bonds are more conformationally sensitive, which is evidenced by their values of the Δ parameter: for the C3'O3', C3'H, C3'C4', C4'C5', C4'O4', C5'O5', and C1'O4' bonds, the Δ value mounts up to 0.004; for the C1'C2', C1'H, C2'C3', C4'H, C5'H1, and C5'H2 bonds, it is equal to 0.003; for the C2'H1, C2'H2, and O5'H bonds, it equals 0.002; and for the O3'H bond, it is 0.001. The more significant flexibility of sugar, as compared to the base part of the nucleoside, is also manifested by the valence angle Δ parameter values. In the base, the valence angle Δ parameter varies from 0.006 (angles N1C2O2 and N3C2O2) to 0.0005 (C4N3H angle). In contrast, in the sugar, the concerned parameter values, on the whole, are much greater: 0.026 for the C2'C3'O3' angle; 0.025 for the O3'C3'H angle; 0.024 for the C4'C3'O3' angle; 0.023 for the O5'C5'H1 angle; 0.022 for the O5'C5'H2 and C4'C5'O5' angles; and 0.004 for the H1C5'H2 angle. Notably, greater flexibility of the sugar against the base part of the nucleosides was also previously observed for some dU conformers²² and quite recently for the T comprehensive family of stable conformers.⁵⁵

To establish correlations between nomenclature conformational parameters, we applied statistical analysis. Strong correlations were found between the δ dihedral angle and the ν_3 (-1.00), ν_2 (0.99), ν_1 (0.94), and ν_4 (-0.92) dihedral angles; the angle ν_1 and the angles ν_2 (0.98) and ν_3 (-0.94); and the angle ν_2 and angles ν_3 (-0.99) and ν_4 (-0.86). The weaker correlations were estimated between the angle ν_1 and angles ν_0 (-0.76) and ν_4 (-0.75), and between the ν_2 angle and the ν_0 (-0.63) angle. There is no correlation between angles ν_0 and ν_3 ; angles ν_0 and ν_4 ; angles γ , ϵ , β , χ , and ν_0 , ν_1 , ν_2 , ν_3 , ν_4 . Again, angles γ , ϵ , β , and χ show no mutual correlation. These findings contradict the crystal-state data,^{1,45} demonstrating rather strong correlation (the correlation coefficient is about 0.78) between χ , ϵ , β , and δ dihedral angles, which probably results from crystal packing forces.

The glycosylic bond length correlates better with the bond lengths within the base (the corresponding coefficients of correlation are N1C2 (-0.80), C5C6 (0.75), C4C5 (-0.73), and

TABLE 1: Structural, Energetic and Polar Characteristics of the dU Conformers According to the MP2/6-311++G(d,p)//DFT B3LYP/6-31G(d,p) Level of Theory

conformer	ΔG^a		d^b	P^c	ν_{\max}^c	χ^c	γ^c	β^c	δ^c	ϵ^c	τ_1^d	τ_2^e	H-bonds ^f
	298.15 K	420 K											
1	0.00	0.00	4.52	161.0	36.3	61.5	45.3	63.4	144.0	-176.3	2.4	3.0	2, 3, 14
2	0.06	0.06	4.47	163.8	36.5	61.6	44.5	64.0	148.9	-65.6	2.1	2.7	2, 3, 14
3	0.59	0.18	7.03	165.4	34.1	-129.9	51.7	176.2	142.8	174.6	1.3	0.7	1, 2, 8
4	0.85	0.01	4.59	138.6	37.9	-120.6	61.0	72.3	131.3	-177.7	-2.5	1.6	1, 10
5	1.21	0.69	2.82	34.9	27.6	65.9	-59.2	169.5	92.8	-62.0	3.5	2.9	4, 6, 11
6	1.30	0.99	4.41	44.0	26.0	62.0	46.0	41.8	93.6	-151.0	1.5	2.6	4, 14
7	1.36	0.95	6.17	13.2	33.9	-159.5	53.2	175.3	84.4	-168.9	1.3	1.0	7, 8
8	1.42	0.81	4.08	147.6	38.4	-171.3	53.1	65.4	137.9	176.8	-0.6	2.0	7
9	1.43	1.05	8.17	167.8	34.0	-126.4	50.9	175.1	147.5	-65.8	-1.5	1.4	1, 2, 8
10	1.50	1.24	3.92	40.1	27.0	60.9	43.7	42.4	95.0	-89.0	1.4	2.4	4, 14
11	1.68	1.00	5.89	48.7	37.7	-123.1	-57.3	178.5	83.5	-55.5	-1.1	1.5	1, 9, 11
12	1.69	1.19	4.41	28.1	32.9	-132.6	64.5	69.7	86.1	-166.4	0.2	0.7	1, 8, 9
13	1.75	1.29	7.18	14.4	34.9	-158.3	50.1	168.1	86.6	-89.9	0.8	1.2	7, 8
14	1.77	1.20	3.96	29.7	25.3	68.4	179.8	-57.8	94.5	-160.1	4.0	3.1	4, 5
15	1.80	1.27	6.21	22.9	36.3	-163.7	-58.7	178.0	83.8	-56.0	0.4	1.4	7, 11
16	1.83	1.26	4.95	30.6	33.5	-129.6	61.9	68.4	89.2	-85.4	0.3	0.7	1, 8, 9
17	1.83	1.41	5.87	171.8	32.7	-125.8	50.5	178.0	139.9	60.1	-1.6	1.4	1, 2, 8
18	1.90	1.19	5.48	147.5	36.8	-114.6	63.6	72.4	140.4	-65.6	-3.4	2.3	1, 10
19	1.97	1.22	4.93	151.5	37.7	-137.4	173.3	-48.2	140.6	178.6	0.5	1.1	1
20	2.02	1.45	3.10	25.8	23.6	67.2	179.3	-56.9	100.0	-84.3	3.6	2.9	4, 5
21	2.05	1.55	5.50	171.4	35.5	63.5	169.8	-60.0	148.8	-178.5	2.8	3.4	3, 5
22	2.12	1.41	5.20	158.2	37.0	-128.2	172.4	-48.0	147.9	-61.9	-0.4	1.4	1
23	2.16	2.04	4.05	165.7	34.3	62.4	42.8	65.4	139.7	47.3	2.2	2.8	2, 3, 14
24	2.27	1.78	3.38	175.2	33.9	65.9	-69.4	174.1	152.1	-65.0	3.5	3.1	3, 6
25	2.34	1.97	6.70	13.3	33.6	-159.1	54.1	179.6	80.6	67.8	1.3	1.0	7, 8
26	2.39	1.68	3.09	18.8	35.5	-165.3	179.4	-54.5	84.1	-174.0	0.9	1.4	7
27	2.39	2.23	4.81	179.4	37.5	56.9	158.9	-71.0	156.6	-59.2	0.8	2.5	3, 5, 14
28	2.40	1.52	6.61	157.7	36.0	-157.2	-69.0	-179.8	145.8	-66.8	1.1	1.9	7
29	2.47	2.02	4.47	38.3	30.0	66.8	-58.8	-77.3	89.5	-67.5	3.8	3.0	4, 11
30	2.56	1.73	4.76	159.6	37.0	-162.3	-64.6	-67.9	144.3	176.9	0.3	1.7	7
31	2.56	2.15	7.29	166.1	34.3	-130.9	53.9	-85.2	143.6	173.1	1.2	0.5	1, 2, 8
32	2.62	2.24	5.96	11.7	35.2	-161.1	54.8	-84.9	82.9	-178.4	1.4	0.9	7, 8
33	2.70	2.24	4.77	26.7	32.7	-132.0	65.0	69.6	82.0	64.2	0.1	0.7	1, 8, 9
34	2.80	2.26	4.83	27.7	24.4	67.4	-179.3	-59.2	90.9	56.5	3.8	3.0	4, 5
35	2.83	2.09	5.07	165.6	36.7	-166.4	-67.4	-177.3	148.0	176.8	0.2	0.9	7
36	2.83	2.38	5.87	24.6	36.9	-163.8	-58.4	-78.5	81.8	-60.7	0.4	1.3	7, 11
37	2.88	2.20	3.47	20.8	35.7	-163.4	-179.5	-56.0	79.4	64.4	0.5	1.0	7
38	2.89	2.37	2.90	151.1	35.8	-130.4	173.6	-49.8	134.8	56.0	0.0	1.1	1
39	2.98	2.26	3.92	22.5	35.7	-163.1	178.6	-53.2	87.8	-80.1	0.3	0.9	7
40	3.04	2.16	6.29	158.6	36.4	-155.3	-67.9	-76.4	146.5	-69.5	1.2	1.9	7
41	3.09	2.34	3.43	137.9	37.8	-166.3	52.4	64.8	126.6	66.6	0.3	1.2	7
42	3.17	2.71	4.73	176.0	34.3	65.8	-67.9	-75.6	152.5	-67.1	3.5	3.0	3, 6
43	3.23	2.89	6.38	12.1	35.0	-160.0	54.1	-85.4	78.9	67.5	1.3	0.9	7, 8
44	3.27	2.75	3.49	173.7	35.0	66.6	-67.1	176.5	150.0	-175.4	4.0	3.4	3, 6
45	3.29	2.37	3.32	186.1	34.3	-145.5	165.7	-31.1	149.1	53.7	1.3	1.4	1, 8, 13
46	3.29	2.93	8.04	169.1	34.5	-127.1	53.5	-83.0	148.8	-60.9	-1.5	1.4	1, 2, 8
47	3.34	3.15	5.98	44.2	25.5	62.0	46.9	40.8	89.6	58.6	1.4	2.6	4, 14
48	3.42	2.92	6.23	192.6	33.8	-163.9	162.7	51.6	151.6	172.6	0.9	1.4	7, 8
49	3.44	2.93	5.99	201.2	33.4	-168.7	171.6	178.8	152.6	172.0	1.6	1.5	7, 8
50	3.55	3.10	4.62	173.5	34.5	66.2	-64.4	-68.7	148.5	-176.6	4.0	3.4	3, 6
51	3.57	3.07	3.25	20.8	38.0	-167.3	-69.8	42.2	77.9	-174.3	-1.5	2.1	7, 12
52	3.60	2.90	3.04	31.9	26.6	67.9	-170.2	-173.2	91.1	-161.5	4.4	3.5	4
53	3.60	3.18	5.83	173.6	33.2	-125.7	52.4	-85.4	141.3	56.9	-1.7	1.4	1, 2, 8
54	3.72	3.40	4.67	215.0	36.4	-169.7	173.4	179.1	152.6	51.4	-2.8	3.1	7, 8
55	3.80	3.39	5.48	209.4	35.2	-166.0	166.4	55.0	150.9	54.6	-1.9	1.8	7, 8
56	3.82	2.98	3.93	194.1	34.3	-169.8	-67.0	-178.6	150.4	54.0	-1.2	2.9	7
57	3.84	2.91	4.33	37.5	34.7	77.0	48.2	168.4	84.6	-101.5	6.2	3.5	4
58	3.89	3.04	4.63	161.7	37.2	-165.7	-74.6	73.0	145.2	172.4	0.3	1.3	7
59	3.91	3.21	2.57	23.9	23.3	66.2	-170.0	-166.6	98.2	-81.5	3.9	3.2	4, 5
60	3.96	3.61	4.23	41.3	35.7	71.0	-69.4	39.9	80.7	-166.4	4.9	3.5	4, 12
61	4.00	3.58	7.00	205.4	33.9	-169.2	173.1	-179.1	157.6	-62.8	-1.9	2.0	7, 8
62	4.02	3.40	5.06	26.8	24.3	67.9	-175.2	64.4	93.1	-160.9	4.4	3.5	4, 5
63	4.03	3.28	4.92	13.2	34.7	-170.3	-174.3	176.2	83.3	-174.8	-2.3	3.9	7
64	4.07	3.24	3.92	27.7	31.8	82.0	53.5	179.4	85.6	-157.8	6.9	3.6	4
65	4.07	3.33	5.15	6.6	33.1	-171.5	178.3	63.7	86.1	-173.5	-2.6	4.9	3, 7
66	4.10	3.65	3.65	22.4	37.8	-165.8	-68.2	50.0	73.7	62.6	-1.1	1.8	7, 12
67	4.15	3.92	4.05	184.7	37.7	57.7	159.6	-73.4	150.9	32.8	0.5	2.4	3, 5, 14
68	4.16	3.65	7.56	195.2	33.8	-162.9	162.4	50.3	156.0	-65.9	0.7	1.2	7, 8
69	4.18	3.74	6.76	12.2	33.7	-161.1	57.0	-80.2	88.6	-79.1	1.2	0.6	7, 8
70	4.31	3.44	4.34	176.5	34.0	-162.8	-64.1	-68.3	144.8	61.1	0.3	0.9	7
71	4.34	3.66	3.59	29.1	25.5	66.9	-169.6	-172.9	87.7	56.5	4.1	3.4	4, 5

TABLE 1 (Continued)

conformer	ΔG^a		d^b	P^c	ν_{\max}^c	χ^c	γ^c	β^c	δ^c	ϵ^c	τ_1^d	τ_2^e	H-bonds ^f
	298.15 K	420 K											
72	4.39	3.67	5.13	16.2	35.0	-168.6	-172.5	177.9	78.2	64.9	-1.9	3.2	7
73	4.42	3.74	4.59	23.3	23.5	66.8	-176.6	59.6	97.3	-90.4	4.1	3.3	4, 5
74	4.61	4.28	4.97	40.6	34.2	69.4	-67.6	50.0	77.8	55.2	4.5	3.4	4, 12
75	4.65	3.81	5.77	9.7	33.3	-170.4	176.8	57.8	89.1	-84.7	-2.2	4.6	7
76	4.71	3.90	6.08	16.9	34.8	-169.0	-173.4	-177.6	86.9	-80.5	-1.8	3.4	7
77	4.74	4.13	4.99	174.1	34.5	66.9	-70.6	88.3	148.7	-179.6	4.2	3.5	3, 6
78	4.85	4.13	5.82	8.7	33.2	-170.2	178.4	65.4	81.5	68.4	-2.4	4.5	7
79	4.92	4.34	1.82	184.7	34.2	68.9	-69.4	172.8	148.1	40.7	3.6	3.4	3, 6
80	5.23	4.26	3.21	176.6	34.1	-163.9	-75.2	74.0	144.3	55.6	-0.1	1.0	7
81	5.29	4.36	5.04	17.9	35.9	-165.5	-74.5	175.7	79.6	48.8	-1.0	1.9	7
82	5.44	4.56	4.07	9.5	31.6	-168.7	-67.5	-175.6	91.2	-167.5	-1.9	3.1	7
83	5.45	4.70	3.40	14.8	19.1	68.1	-68.5	167.7	97.8	48.5	3.3	3.2	4, 6
84	5.47	4.90	5.84	23.3	23.0	67.4	-175.8	67.3	90.3	59.7	4.1	3.4	4, 5
85	5.48	4.98	4.02	184.5	33.5	68.8	-64.7	-68.7	146.4	47.4	3.7	3.4	3, 6
86	5.83	5.34	6.06	175.5	32.7	67.4	180.0	60.5	145.7	179.9	5.2	3.6	3, 5
87	5.85	5.37	5.97	179.5	33.5	68.0	179.6	60.4	151.5	-63.6	4.9	3.3	3, 5
88	5.95	5.21	5.42	28.1	30.6	80.9	56.0	-172.7	82.4	61.9	6.9	3.6	4
89	5.97	5.39	5.86	11.0	17.3	69.0	-54.3	-53.2	98.6	61.9	3.4	3.3	4, 6
90	5.99	4.26	3.32	185.7	33.9	69.4	-72.9	87.1	147.1	38.7	3.8	3.5	3, 6
91	7.19	6.61	4.66	191.7	32.1	72.1	179.0	62.5	144.9	48.0	4.9	3.6	3, 5
92	7.46	6.75	6.15	150.4	40.0	78.4	50.5	-81.0	138.1	177.9	6.4	3.7	3
93	7.60	6.80	6.43	156.4	38.5	77.1	53.5	-74.1	144.3	-61.6	6.4	3.2	3
94	8.96	7.91	4.90	155.1	35.4	77.8	53.1	-78.2	133.6	54.0	6.5	3.7	3

^a Relative free Gibbs energy at $T = 298.15$ K and $p = 1.00$ atm (kcal/mol). ^b Dipole moment (D). ^c For definition of the conformational angles, see Figure 1 and ref 1. ^d Angle between the C1'N1 bond and the mean base plane. ^e Maximum of torsion angles in the base. ^f For definition of the H-bond types, see Table 5.

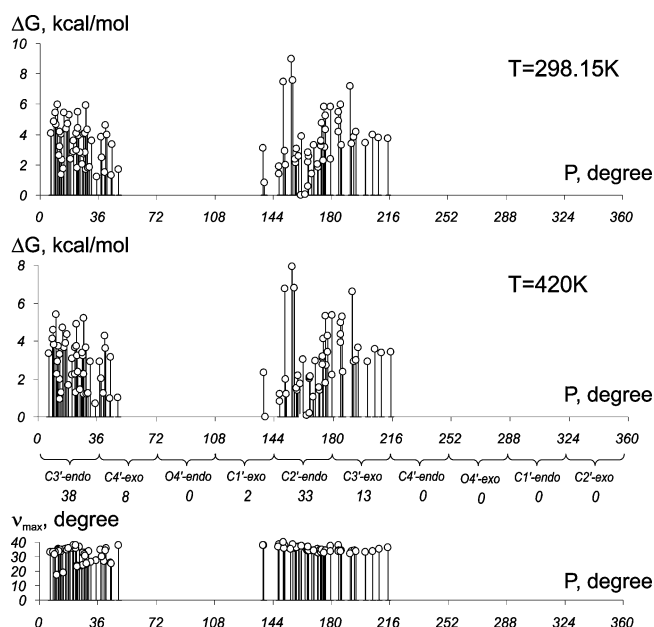


Figure 2. Distribution of 94 found conformers of dU with regard to relative free Gibbs energy ΔG at 298.15 and 420 K, as well as the puckering amplitude ν_{\max} as a function of pseudorotational phase P .

N3C4 (0.71)) than with those within the sugar residue, where the maximal correlation is established for the C1'O4' bond length (-0.63). The similar situation is observed for the correlation between the C1'N1 bond length and bond angles of the base and sugar: a better correlation is observed for bond angles of the base, namely, C4N3H (0.84), C2N3C4 (-0.72), N1C2O2 (-0.72), and N1C2N3 (0.71). In the case of the sugar, the maximal correlation was found for the C3'C2'H2 bond angle and equals 0.68. The glycosidic bond also correlates with dihedral angles within the sugar residue (C4'O4'C1'N1 (0.86), C4'O4'C1'H (0.83), and ν_0 (-0.82)). Contrary to the data of

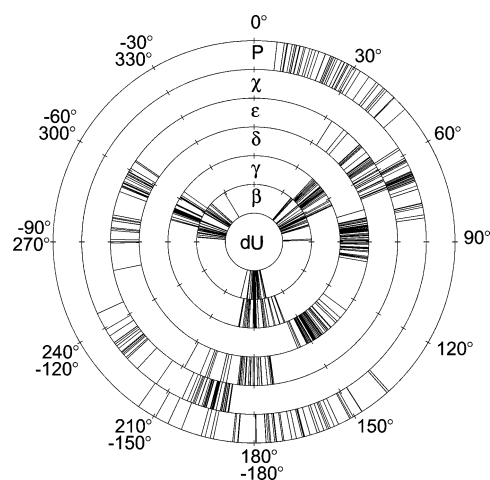


Figure 3. Conformation wheel for the main structural parameters (P , χ , ϵ , δ , γ , β) of a dU molecule.

the earlier crystal-state studies of pyrimidine nucleosides,¹ we did not find a correlation between values of the glycoside bond length and the χ angle.

Our findings show that χ correlates with the following parameters: bond lengths N1C6 (0.86) and C5C6 (0.85); bond angles C2N1C6 (-0.96), C4C5H (0.95), C1'N1C2, N1C6C5 (0.94), and C5C6H (-0.94); and dihedral angles C2'C1'N1C6 (1.00), N3C4C5H, C4C5C6H (0.99), N1C6C5H (-0.97), O4C4C5H (0.95), C2'C1'N1C2 (-0.95), C6N1C1'H (0.94), and O4'C1'N1C6 (-0.94).

In the full conformational family of dU, there are three DNA-like conformers, *videlicet*, conformers **3**, **7**, and **9**, corresponding to the BI^{1,56,57} ($\chi \in \text{anti}$, $P \in \text{C2' endo}$, $\beta \in \text{t}$, $\gamma \in \text{g}^+$, $\epsilon \in \text{t}$), AI^{1,58} ($\chi \in \text{anti}$, $P \in \text{C3' endo}$, $\beta \in \text{t}$, $\gamma \in \text{g}^+$, $\epsilon \in \text{t}$) and BI^{1,56,57} ($\chi \in \text{anti}$, $P \in \text{C2' endo}$, $\beta \in \text{t}$, $\gamma \in \text{g}^+$, $\epsilon \in \text{g}^-$) DNA forms, respectively (Table 3, Figure 4). Conformer **13** ($\chi \in \text{anti}$, $P \in \text{C3' endo}$, $\beta \in \text{t}$, $\gamma \in \text{g}^+$, $\epsilon \in \text{g}^-$) might be relative to a

TABLE 2: Some Structural Data of dU from X-ray Data and DFT Calculations^a

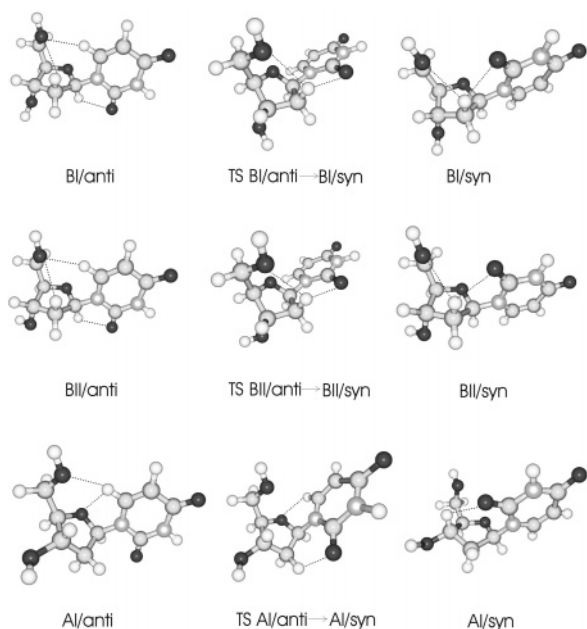
conformer	<i>P</i>	ν_{\max}	χ	ν_0	ν_1	ν_2	ν_3	ν_4	γ	δ	β	ϵ	C6N1- C2N3	N1C2- N3C4	C2N3- C4C5	N3C4- C5C6	C4C5- C6N1	C5C6- N1C2	τ_1^b
28^c	157.7	36.0	-157.2	-24.2	36.1	-33.3	20.4	2.2	-69.0	145.8	-179.8	-66.8	-1.5	1.9	-1.2	0.1	0.1	0.6	1.1
M1^d	172.9	37.8	-153.6	-16.8	33.9	-37.5	28.8	-7.6	-69.2	156.6	t	g-	-4.0	1.8	1.9	-3.8	1.8	2.4	2.9
M2^d	177.7	35.3	-156.5	-13.0	31.1	-35.3	28.9	-10.9	-74.4	158.9	t	g-	-2.6	2.0	-0.3	-0.9	0.3	1.6	2.8

^a Definitions of angles are as in Figure 1 and ref 1. ^b Angle between the C1'N1 bond and the mean base plane. Angles are given in degrees. ^c Calculated conformer **28** (see Table 1). ^d The pair of coexisting conformers Molecule 1 (**M1**) and Molecule 2 (**M2**) evidenced from X-ray data.⁵ Experimental data are insufficient for estimation of exact values of β and ϵ angles, but allow one to determine the sectors they occupy.

TABLE 3: Structural and Energetic Characteristics of Biologically Important dU and T Conformations

nucleoside	conformation	ΔG^a	$\Delta \Delta G^b$	<i>P</i> ^c	ν_{\max}^c	χ^c	γ^c	δ^c	β^c	ϵ^c	<i>l</i> ^d	τ_1^e	τ_2^e
dU	BI/anti	0.59		165.4	34.1	-129.9	51.7	142.8	176.2	174.6	1.465	1.3	0.7
	TS/anti → syn	6.61	6.02	151.8	41.3	110.2	46.0	140.1	167.6	178.5	1.467	0.6	3.8
	BI/syn	4.91		153.4	39.4	71.0	42.2	140.0	180.0	180.0	1.464	-3.7	4.9
	BII/anti	1.43		167.8	34.0	-126.4	50.9	147.5	175.1	-65.8	1.464	-1.5	1.4
	TS/anti → syn	7.28	5.85	158.1	40.1	114.4	46.0	146.8	165.7	-68.0	1.470	0.4	3.1
	BII/syn	5.19		157.7	38.9	69.4	39.7	145.7	180.0	-67.1	1.465	-3.3	4.4
	AI/anti	1.36		13.2	33.9	-159.5	53.2	84.4	175.3	-168.9	1.490	1.3	1.0
	TS/anti → syn	5.67	4.31	335.0	38.2	142.2	54.0	95.4	176.6	-167.7	1.507	-1.3	3.2
	AI/syn	4.07		27.7	31.8	82.0	53.5	85.6	179.4	-157.8	1.477	-2.6	4.9
T	BI/anti	0.65		164.6	34.4	-129.5	51.3	142.7	176.2	174.1	1.464	1.1	-0.8
	TS/anti → syn	6.76	6.11	151.7	41.3	110.2	45.9	140.0	167.6	178.0	1.466	3.8	-0.6
	BI/syn	4.73		152.8	39.4	71.7	42.7	139.6	180.0	180.0	1.463	5.4	-3.4
	BII/anti	1.38		167.2	34.2	-125.6	50.3	147.3	174.9	-65.4	1.463	-1.4	-1.6
	TS/anti → syn	7.42	6.04	157.0	40.3	113.7	45.7	146.3	165.3	-67.9	1.468	3.0	0.2
	BII/syn	5.21		156.9	38.9	69.4	40.0	145.2	180.0	-66.9	1.464	4.6	-3.0
	AI/anti	1.34		13.7	34.2	-158.8	52.9	84.0	175.6	-168.8	1.488	0.9	1.1
	TS/anti → syn	5.93	4.59	336.1	38.0	143.2	53.7	94.9	177.6	-168.3	1.506	3.4	1.7
	AI/syn	4.21		28.3	31.8	81.8	53.5	85.5	179.5	-158.1	1.476	7.1	-3.9

^a Relative Gibbs energy (kcal/mol) at 298.15 K. ^b Anti → syn transition state Gibbs energy (kcal/mol) at 298.15K. ^c For the definition of these conformational angles, see Figure 1 and ref 1. ^d Glycosidic bond length C1'N1 (Å). ^e For the definition of these conformational parameters, see footnote of Table 1. TS/anti → syn denotes the transition state between anti and syn DNA-like conformers. BI/syn and BII/syn conformations of dU and T were obtained by optimizing geometries with a constrained torsional angle β at 180°. ³⁰ All geometries were calculated at the B3LYP/6-31G(d,p) level of theory, whereas energetic characteristics were calculated at the MP2/6-311++G(d,p)/B3LYP/6-31G(d,p) level of theory.

**Figure 4.** Spatial structure of biologically important conformations of dU. Intramolecular H-bonds are denoted by dotted lines (see also Tables 3, 4).

hypothetical AII form of DNA, although it has not yet been discovered. At 298.15 K, conformer **3** appears to be the most energetically favorable in the anti subfamily (Table 1).

Earlier it was shown that DNA glycosylases, before excision (through heterolytic opening of the glycosylic bond)⁵⁹ of dU

and T, improperly paired with 2'-deoxyguanosine (dG), force bases to flip out from a double strand, i.e., subject them to the anti → syn conformational transition.^{60–62} Here, we have investigated the dU and T transition states (TS) of the anti → syn interconversion. In Table 3, energies and conformational parameters of the DNA-like conformers of dU and T (Figure 4) in anti and syn conformations are compared with the same characteristics of TS. Since flipped-out syn conformation of the pyrimidine nucleosides is believed to be a transition state in enzymatic excision of mispaired dU,⁶² our calculated anti → syn TS might be regarded as a pre-transition state.

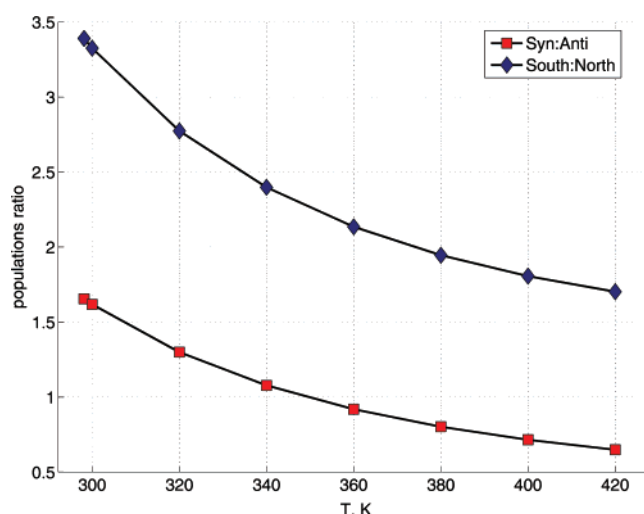
On the basis of close similarity between energetic and structural features of DNA-like conformers of dU and thymidine and their anti → syn interconversion TS, we suppose that the difference in the shape of the bases' residues, rather than the electronic⁶³ influence of the bulky methyl group in T, contributes to the mismatch glycosylase discrimination between the mispaired dU and rightly paired T with 2'-deoxyadenosine (dA) in the course of the dU reparative excision from DNA.

The fact that the largest elongation of the glycosylic bond (0.017 Å for dU and 0.018 Å for T) in the TS of the A form conformers, characterized by two stabilizing hydrogen bonds C2'H2...O2 and C6H...O4' and closed-shell contacts⁶⁴ between the N1 and O5' atoms (Figure 4, Tables 3, 4) along with the lowest energetic barrier of the anti → syn interconversion TS (4.31 and 4.59 kcal/mol for dU and T, respectively), suggests that, in the glycosylase active site, the nucleoside might first be put in shape relative to the DNA A form, which might forestall the base elimination via opening the N1–C1' valence bond. In other words, we cannot reject the possibility that

TABLE 4: AIM Characteristics of Intramolecular Interactions in the dU and T DNA-like Conformer anti \rightarrow syn Transition States

nucleoside	DNA form	interaction	ρ^a	$\nabla^2\rho^b$
dU	BI	C2'H2...O2	0.018	0.067
		C2'H2...O5'	0.008	0.033
	BII	C2'H2...O2	0.018	0.068
		C2'H2...O5'	0.009	0.037
	AI	C2'H2...O2	0.022	0.076
		C6H...O4'	0.018	0.083
T	BI	N1...O5'	0.007	0.024
		C2'H2...O2	0.018	0.067
	BII	C2'H2...O5'	0.008	0.033
		C2'H2...O2	0.018	0.068
	AI	C2'H2...O5'	0.009	0.036
		C2'H2...O2	0.022	0.076
		C6H...O4'	0.018	0.080
		N1...O5'	0.006	0.022

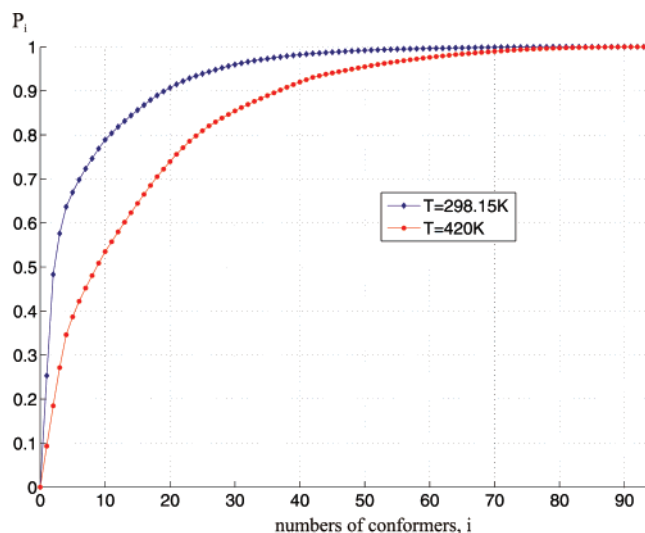
^a The electron density value at the BCP. ^b The Laplacian of electron density value at BCP. All units are atomic units. All wavefunctions are calculated at the DFT B3LYP/6-31G(d,p) level of theory.

**Figure 5.** Dependence of syn/anti and N/S equilibrium on temperature.

glycosylases, at least some of them, might transform the pyrimidine nucleosides from the B to the A form of DNA in the course of the excision initiation, especially since intimate processes of reparative excision are yet insufficiently studied and elucidated in literature.

Temperature Dependence of dU Conformational Equilibrium. The conformational equilibrium of dU was calculated for the range of temperature from 298.15 to 420 K, taking into account all the conformers. For the main structural parameters χ and P , conformational equilibrium essentially depends on temperature (Figure 5). Thus, at 298.15 K, the populations of syn bases and S sugars dominate (syn/anti = 62.3%:37.7% and S/N = 77.2%:22.8%), but at 420 K, anti conformers dominate, and the contribution of S conformers decreases (syn/anti = 39.3%:60.7% and S/N = 63.0%:37.0%). According to Figure 5, at 349 K, anti and syn conformers appear to be equally populated. The 90% tolerance in determining conformational equilibrium can be achieved taking into account only the first 21 conformers at 298.15 K and 38 at 420 K. To guarantee 5% tolerance, 29 conformers at 298.15 K and 50 conformers at 420 K should be considered.

It should be noted that the first 20 and 37 conformers provide 90% of the total population at 298.15 and 420 K, respectively. To achieve 95% of the total population, 28 and 49 conformers at 298.15 and 420 K should be taken into account, respectively (Figure 6).

**Figure 6.** Dependence of relative integral population P_i of i , the most energetically favorable conformers, on their number i at 298.15 and 420 K ($P_i = \sum_{n=1}^i p_n$, where $i = 1...94$).

In addition, the occurrence frequency of the sugar pucker types at 298.15 K was considered, depending on parameters P and χ . For S and N conformers, the following sugar pucker occupancies were established: the S conformers C2'-endo 70.6%, C1'-exo 6.2%, and C3'-exo 0.5%; the N conformers C3'-endo 15.8% and C4'-exo 6.9%.

The C2'-endo pucker of the sugar occurs mainly in the syn conformers (syn – 51.1% against anti – 19.5%), as well as C4'-exo (syn – 5.4% against anti – 1.5%). The C3'-endo sugar pucker is predominantly connected with the anti orientation of the base (anti – 10.1% against syn – 5.8%), and the C1'-exo is observed only in the anti conformers contributing to the total population 6.2%. The C3'-exo sugar pucker occurs in 0.4% of anti and 0.03% of syn conformers. Our results demonstrate that, in addition to the C2'-endo and C3'-endo traditional conformations of the sugar, which came from X-ray¹ and NMR^{1,11} data, there are other types of the sugar moiety puckering appreciably contributing to the general population of dU.

Intramolecular Hydrogen Bonds. On the whole, in 94 conformers of dU, 175 intramolecular H-bonds were established, classified into 14 types of H-bonds (Table 5), namely, C1'H...O2 (16 H-bonds), C2'H2...O5' (9), C2'H2...O2 (21), C3'H...O2 (21), C5'H1...O2 (14), C5'H2...O2 (11), C6H...O4' (37), C6H...O5' (22), C3'H...HC6 (4), O5'H...HC6 (2), O3'H...O5' (5), O5'H...O4' (1), O5'H...O3' (4), and O5'H...O2 (8). Among them, H-bonds of types 1, 3, 4, 5, 6, 7, 8, 9, 10, and 14 (the whole number 156) are formed between atomic groups of base and sugar; H-bond types 2, 11, 12, and 13 (in amounts 19), localized inside the sugar residue and detected also in model sugar residues of 2'-deoxyribonucleosides,³⁹ appeared to be very sensitive to the sugar–base mutual orientation. Notably, the H-bond types 1, 7, 8, 9, and 10 can be formed in anti conformers only, and the 4, 5, 6, and 14 types are only formed in syn conformations (Table 6). All H-bonds inside the deoxyribose residue prefer conformers with anti-oriented base, except the H-bonds of the type 12, which proved to be indifferent to both syn and anti conformations. These H-bonds are sensitive to the sugar conformation: types 2 and 13 can be formed only in S conformations, types 11 and 12 only in N conformations.

Among H-bonds between the base and sugar residue, the most sensitive to sugar conformations are H-bonds of the 3, 4, 9, and 10 types: types 3 and 10 are formed only in S conformations (there is only one exception inside type 3), H-bonds of

TABLE 5: Minimal and Maximal Geometrical and Topological Characteristics of Intramolecular H-bonds Types in dU

H-bond type	H-bond AH...B	AB ^a		HB ^b		AHB ^c		ρ^d		$\nabla^2\rho^e$	
		min	max	min	max	min	max	min	max	min	max
1	C1'H...O2	2.732	2.784	2.211	2.268	103.1	109.3	0.005	0.020	0.019	0.082
2	C2'H2...O5'	3.106	3.231	2.584	2.702	108.3	110.2	0.008	0.009	0.030	0.035
3	C2'H2...O2	2.905	3.134	2.144	2.531	106.6	125.6	0.008	0.021	0.028	0.068
4	C3'H...O2	2.964	3.136	2.363	2.613	108.1	116.9	0.008	0.013	0.034	0.050
5	C5'H1...O2	3.038	3.686	2.305	2.942	105.0	144.2	0.004	0.013	0.016	0.043
6	C5'H2...O2	3.246	3.699	2.378	2.966	124.4	135.3	0.004	0.012	0.015	0.039
7	C6H...O4'	2.683	2.742	2.216	2.325	100.7	104.0	0.017	0.020	0.072	0.078
8	C6H...O5'	3.286	3.709	2.260	2.671	147.8	164.0	0.007	0.015	0.027	0.042
9	C3'H...HC6	2.918	3.016	2.349	2.466	109.3	110.6	0.005	0.006	0.018	0.023
10	O5'H...HC6	2.787	2.957	2.213	2.304	116.9	124.2	0.006	0.019	0.025	0.077
11	O3'H...O5'	2.918	3.071	2.185	2.406	125.4	131.3	0.012	0.016	0.041	0.053
12	O5'H...O3'	2.978	3.025	2.179	2.264	134.6	140.1	0.015	0.017	0.047	0.051
13	O5'H...O4'	2.735	2.735	2.157	2.157	116.8	116.8	0.019	0.019	0.076	0.076
14	O5'H...O2	2.818	3.012	1.863	2.199	140.5	166.4	0.015	0.028	0.047	0.091

^a Distance between A (donor) and B (acceptor) atoms. ^b Distance between H and B atoms. ^c H-bond angle. ^d The electron density value at BCP. ^e The Laplacian of electron density value at BCP. Distances are given in angstroms, angles in degrees, electron density, and Laplacian of electron density in atomic units. All the characteristics are calculated at the DFT B3LYP/6-31G(d,p) level of theory.

TABLE 6: Conformational Characteristics of Intramolecular H-bonds in dU

H-bond type	H-bond AH...B	number of H-bonds					β^a			γ^a			ϵ^a		
			syn	anti	north	south	g ⁺	t	g ⁻	g ⁺	t	g ⁻	g ⁺	t	g ⁻
1	C1'H...O2	16	0	16	4	12	5	4	7	11	4	1	5	5	6
2	C2'H2...O5'	9	3	6	0	9	3	3	3	9	0	0	3	3	3
3	C2'H2...O2	21	20	1	1	20	9	3	9	6	7	8	7	8	6
4	C3'H...O2	21	21	0	21	0	8	8	5	6	9	6	8	6	7
5	C5'H1...O2	14	14	0	8	6	6	2	6	0	14	0	5	4	5
6	C5'H2...O2	11	11	0	3	8	2	5	4	0	0	11	5	3	3
7	C6H...O4'	37	0	37	21	16	12	15	10	8	15	14	13	13	11
8	C6H...O5'	22	0	22	9	13	6	9	7	15	7	0	8	7	7
9	C3'H...HC6	4	0	4	4	0	3	1	0	3	0	1	1	1	2
10	O5'H...HC6	2	0	2	0	2	2	0	0	2	0	0	0	1	1
11	O3'H...O5'	5	2	3	5	0	0	3	2	0	0	5	0	0	5
12	O5'H...O3'	4	2	2	4	0	4	0	0	0	0	4	2	2	0
13	O5'H...O4'	1	0	1	0	1	0	0	1	0	1	0	1	0	0
14	O5'H...O2	8	8	0	3	5	6	0	2	6	2	0	3	2	3

^a For the definition of the conformational angles, see Figure 1 and ref 1.

types 4 and 9 were found in N conformations of the sugar residue. H-bonds of types 1, 6, 8, and 14 prevail in S conformations; in contrast, H-bonds of types 5 and in 7 prefer N conformations.

Conformational parameters γ , β , and ϵ were shown to determine the formation of some H-bonds. Thus, H-bonds of the types 2 and 10 can be formed only if $\gamma \in g^+$; 6, 11, and 12 can only be formed if $\gamma \in g^-$; 5 and 13 can only be formed if $\gamma \in t$. The H-bonds of the type 10 and 12, localized inside the sugar residue, impose the most stringent requirements on the nucleoside conformation: their formations are realized if $\beta \in t, g^-$, $\gamma \in g^-$, $\epsilon \in g^-$ and $\beta \in g^+$, $\gamma \in g^-$, $\epsilon \in g^+, t$, correspondingly.

The most dU conformers are shaped by more than one H-bond. Seventeen conformers (6 syn and 11 anti) are stabilized by three H-bonds, 47 conformers (28 syn and 19 anti) are stabilized by two H-bonds, and 30 conformers (7 syn and 19 anti) are stabilized by one H-bond. No conformers without H-bonds were found.

Among the four H-bond types detected in all possible conformers of dU (OH...O, CH...O, OH...HC, and CH...HC), special attention should be focused on the last two types, i.e., hydrogen-hydrogen bonds. Their distinctive feature consists in the fact that hydrogen atoms from different CH and OH groups may act as H-bond donors and acceptors at the same time. These H-bonds were detected in nucleosides for the first time. Earlier these H-bonds were detected in some amino acids⁶⁵ by the Bader's electron density topological method.⁴⁷ Such

H-bonds were first reported in the literature for interactions of neutral and deprotonated water molecules.⁶⁶ Now the study of these H-bonds is proceeding vigorously, mainly by methods of ab initio quantum chemistry.⁶⁷

It should be emphasized that 95% of H-bonds correspond to the classical criteria of H-bonding: the sum of van der Waals radii of H and B atoms should not exceed the HB distance (the above-mentioned value for H and O or H and H equals 2.72 and 2.40 Å correspondingly).⁶⁸ The minimal value of the AHB angle of H-bonding equals 100.7° for C6H...O4' hydrogen bonds (Table 5). Values of electron density ρ and the Laplacian of electron density $\nabla^2\rho$ also lie within the Koch and Popelier's ranges⁴⁸ (Table 5). We have shown earlier³⁸ that even the weakest of the nontraditional CH...O/N interactions in nucleosides can be classified as true hydrogen bonds, since they satisfy all eight of the criteria of Koch and Popelier.⁴⁸

The great number of H-bonds enabled us to apply statistic method—correlation analysis. Rather strong correlation between the electron density ρ and Laplacian $\nabla^2\rho$ is established (the correlation coefficient is 0.94). There are also correlations between ρ and HB distance (the correlation coefficient equals 0.87), $\nabla^2\rho$ and HB distance (0.74), and $\nabla^2\rho$ and AB distance (0.85). These data show clearly that ρ and $\nabla^2\rho$ parameters characterize the strength of H-bonds, which is in agreement with results.^{50,51}

We evaluated the strength of intramolecular OH...O hydrogen bonds using the Grabowski complex measure Δ_{com} . As a result, the OH...O H-bonds in dU conformers fall into the 0.012–

TABLE 7: Structural, Vibrational, and Energetic Data on the Traditional Intramolecular OH...O Hydrogen Bonds in dU Conformers

conformer	H-bond AH...B	AB ^a	HB ^b	AHB ^c	Δ_{AH}^d	$\Delta\nu_{\text{str}}^e$	$I_{\text{str}}/I_{\text{ostr}}^f$	Δ_{com}^g	$-\Delta H^h$
1	O5'H...O2	2.847	1.895	165.2	0.009	146	41.7	0.036	3.40
2		2.827	1.871	166.3	0.010	154	45.6	0.037	3.52
6		2.935	2.048	150.8	0.007	101	22.8	0.027	2.58
10		2.920	2.023	152.6	0.007	111	25.6	0.028	2.78
23		2.818	1.863	166.4	0.009	144	44.9	0.036	3.37
27		3.012	2.199	140.5	0.005	65	11.7	0.024	1.65
47		2.925	2.036	151.2	0.007	101	23.9	0.025	2.58
67		2.967	2.154	140.5	0.005	64	12.2	0.024	1.62
51	O5'H...O3'	2.978	2.179	138.7	0.005	82	7.1	0.015	2.14
60		2.995	2.186	140.1	0.005	83	7.2	0.016	2.16
66		3.005	2.232	135.8	0.005	83	5.9	0.015	2.16
74		3.025	2.264	134.6	0.005	78	5.3	0.014	2.03
5	O3'H...O5'	3.021	2.340	126.7	0.004	64	8.3	0.013	1.62
11		2.918	2.185	131.3	0.005	80	12.2	0.017	2.09
15		2.928	2.201	130.8	0.005	76	11.2	0.016	1.98
29		3.071	2.406	125.4	0.004	63	7.5	0.012	1.58
35		2.986	2.269	129.9	0.005	82	10.0	0.017	2.14
46	O5'H...O4'	2.735	2.157	116.8	0.004	59	3.9	0.013	1.44

^a Distance between A (donor) and B (acceptor) atoms. ^b Distance between H and B atoms. ^c H-bond angle. ^d Difference between the AH distances in the presence of the H-bond and in the nonbonded state. ^e Decrease in AH stretching mode frequency upon H-bonding. ^f I_{str} and I_{ostr} : AH stretching mode integral intensity upon H-bonding and in the nonbonded state, respectively. ^g Measure of H-bond strength according to Grabowski.^{50,51} ^h H-bond energy calculated after Iogansen.⁵² Distances are given in angstroms, angles in degrees, frequencies in cm^{-1} , energy values in kcal/mol. Frequencies are calculated at the DFT B3LYP/6-31G(d,p) level of theory in harmonic approximation and are scaled (scaling factor 0.9485).

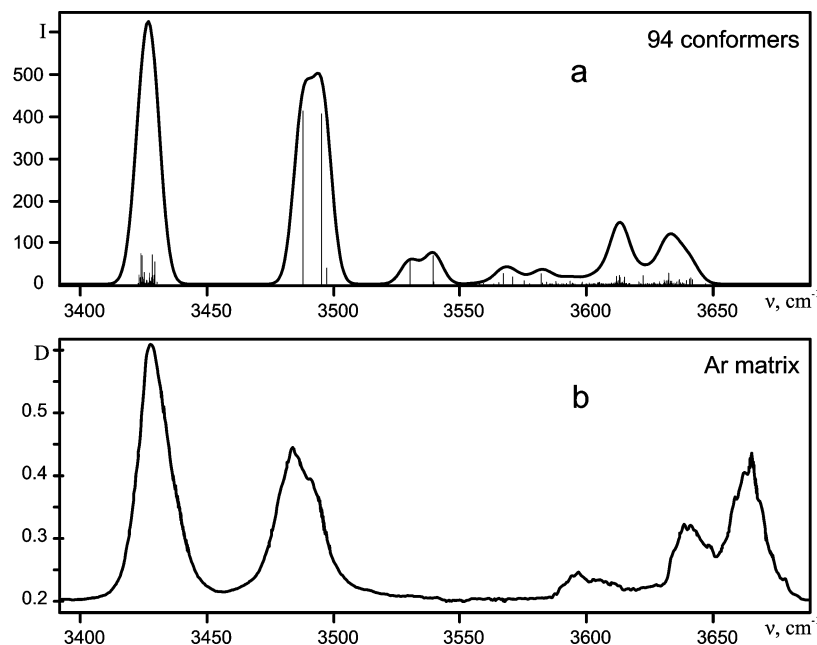


Figure 7. (a) IR calculated spectrum of dU. Intensities are given in km/mol . Spectral contributions of individual conformers are approximated by Gaussian functions with the 8.5 cm^{-1} halfwidth, which guarantees the smooth resulted spectrum. (b) experimental low-temperature matrix spectrum.²⁰

$0.037 \Delta_{\text{com}}$ range. The rather strong correlation between Δ_{com} and H-bond energy $-\Delta H$ (the correlation coefficient equals 0.92) proves that Δ_{com} can be efficiently used for the evaluation of ΔH .

So, our results demonstrate a very complicated integral system of intramolecular H-bonding, shaping nucleosides, which in part were studied earlier.^{22,69,70}

IR Spectrum of dU Calculated at 420 K. The OH stretching vibrations ($3400\text{--}3700 \text{ cm}^{-1}$) of isolated nucleosides are believed to be the most conformationally sensitive in IR spectra,²⁰ which originates mainly from intramolecular H-bonds. Table 7, displays traditional intramolecular OH...O hydrogen bonds in dU conformers. In Figure 7 we present the calculated spectrum (convolution of all 94 individual spectra of conformers populated by Boltzmann's rule) and, for comparison, the low-

temperature argon matrix IR spectrum according to data,²⁰ respectively.

The lowest frequency band (the 3428 cm^{-1} band), corresponding to the N3H bond stretch, appeared to be insensitive to the nucleoside conformation. An appropriate choice of scale factor brought this band frequency into accord with the experimental value. The intense doublet at $3490/3498 \text{ cm}^{-1}$ is determined by stretching vibrations of O5'H hydroxyl groups involved into the O5'H...O2 hydrogen bonds in S/syn conformers **3** and **2**, the most energetically favorable in syn family. The much less intensive doublet at $3533/3543 \text{ cm}^{-1}$ corresponds to the same vibrations of N/syn conformers **16** and **6**. Different orientations of O3'H hydroxyl groups are responsible for the average 9 cm^{-1} splitting of the above two bands. In the IR spectrum of dU, isolated in an argon matrix, the intensive band

at 3482 cm^{-1} with a shoulder at $\sim 3492\text{ cm}^{-1}$ evidently corresponds to the first of the above two doublets, and is non-resolved because of interactions with the matrix, whereas the absorption in the $3515\text{--}3550\text{ cm}^{-1}$ region, very broadened by the matrix effect, may be assigned to the second doublet at $3533/3543\text{ cm}^{-1}$. The calculated band at 3572 cm^{-1} is determined mainly by the stretching vibrations of the O3'H hydroxyl groups involved in the O3'H...O5' hydrogen bonds of the N/anti conformers and correlates with the experimental broad band with a peak at 3598 cm^{-1} . In the case of N/syn conformers, the same vibrations contribute to the calculated band at 3586 cm^{-1} as well as vibrations of free O5'H and O3'H hydroxyl groups in some S/anti and N/anti conformers, correspondingly. In experimental spectra, these vibrations give rise to broad absorption at $\sim 3608\text{ cm}^{-1}$. As is easy to see, the 14 cm^{-1} gap separates vibrations of H-bonded O3'H groups in N/syn and N/anti conformers. Notably, stretching vibrations of hydroxyl groups of two types in the nucleoside display dependence on different conformational parameters: $\nu(\text{O5'H})$ s are sensitive to P , while $\nu(\text{O3'H})$ s are sensitive to χ , but not to P .

Above this region, the spectrum exclusively reflects vibrations of free hydroxyl groups. The 3615 cm^{-1} (experimental value 3641 cm^{-1}) band is a superposition of major contribution of the O3'H hydroxyl groups in S/anti,syn conformers and minor contribution from the O5'H groups' vibrations, for the most part, in S,N/anti conformers. The 3635 cm^{-1} band is determined mainly by stretching vibrations of O3'H free groups in N/anti,syn conformers and O5'H free groups' vibrations of conformers with various combinations of parameters P and χ . Stretching vibrations of the O5'H and O3'H free groups in some N/syn conformers are responsible for the high frequency shoulder at 3645 cm^{-1} of the band at 3635 cm^{-1} . The rather intensive experimental band at 3665 cm^{-1} unites these vibrations.

It will readily be seen that the O5'H...O2 hydrogen bonds are the strongest ones (Table 7), thus, they substantially influence the IR spectrum of dU. In contrast, the O5'H...O3' hydrogen bonds, appearing in high-energy conformers, contribute negligibly to the general landscape of the spectrum. So, the IR spectrum calculated at 420 K reproduces the low temperature argon matrix spectrum obtained at the same temperature of evaporation with a wavenumber discrepancy not exceeding 1%, which shows the reliability of our approach to conformational analysis of dU.

IV. Concluding Remarks

A comprehensive approach to conformational analysis of nucleosides, canonical,⁵⁵ modified,³⁸ and minor (this work), provides new insight to the nature of these biologically important molecules. Nucleosides, particularly deoxyribonucleosides, are extremely flexible: they can adopt dozens (up to hundreds) of stable conformation shaped by a rather complicated system of intramolecular H-bonding. This fact, estimated theoretically, agrees well with significant inhomogeneous broadening of absorption bands in the IR spectra of nucleosides, isolated in a low-temperature matrix.^{20,21} The high flexibility of sugar residues in nucleosides evidently plays an important part in conformational transitions in DNA and its deformation in the course of biochemical reactions, e.g., DNA synthesis and reparation.

The close similarity of the energetic and structural features of the dU and T DNA-like conformers along with their anti \rightarrow syn interconversion TS gives evidence in favor of the suggestion that mainly difference in the base shapes contributes to the mismatch glycosylase discrimination between dU and T, but not the electronic⁶³ influence of the T methyl group.

The ab initio theoretical procedure described in this work has proven its reliability to satisfactorily reproduce the IR spectrum of dU isolated in a low-temperature matrix. This approach can be undoubtedly applied to other isolated deoxy- and ribonucleosides and offers the possibility of theoretical interpretation of their spectra, whatever the temperature is, particularly a physiological one.

Acknowledgment. This work was prepared in the framework of a scientific collaboration between the Institute of Molecular Biology and Genetics, the National Academy of Sciences of Ukraine, and BioMoCeTi (UMR CNRS 7033). Y.P.Y. was granted as a Ph.D. fellow from the French Embassy in Ukraine. The authors would also like to thank the French calculation center CINES (Montpellier, France) for the computational facilities on the IBM SP3 workstations. The authors from Kyiv greatly appreciate the valuable technical assistance of Dr. Andriy L. Potyahaylo.

References and Notes

- (1) Saenger, W. *Principles of Nucleic Acid Structure*; Springer-Verlag: New York, 1984.
- (2) Rahman, A.; Wilson, H. R. *Nature* **1971**, 232, 333.
- (3) Sundaralingam, M. *Ann. N. Y. Acad. Sci.* **1976**, 255, 3.
- (4) Lavut, Ye. E.; Zorkiy, P. M.; Chernikova, Yu. N. *Zh. Strukt. Khim. (Russian)* **1981**, 22, 89.
- (5) Rahman, A.; Wilson, H. R. *Acta Crystallogr.* **1973**, B28, 2260.
- (6) Rozenberg, M.; Jung, C.; Shoham, G. *Phys. Chem. Chem. Phys.* **2003**, 5, 1533.
- (7) Zhizhina, G. P.; Oleinik, E. F. *Usp. Khim. (Russian)* **1972**, 41, 258.
- (8) Peticolas, W. L. In *Methods in Structural Molecular Biology*; Davies, D. B., Saenger, W., Danyluk, S. S., Eds.; Plenum Press: London, 1981; pp 161–213.
- (9) Gaigeot, M. P.; Leulliot, N.; Ghomi, M.; Jobic, H.; Coulombeau, C.; Bouloussa, O. *Chem. Phys.* **2000**, 261, 217.
- (10) Leulliot, N.; Ghomi, M.; Jobic, H.; Bouloussa, O.; Baumruk, V.; Coulombeau, C. *J. Phys. Chem. B* **1999**, 103, 10934.
- (11) Davies, D. B. *Prog. Nucl. Magn. Reson. Spectrosc.* **1978**, 12, 135.
- (12) Markowski, V.; Sullivan, G. R.; Roberts, J. D. *J. Am. Chem. Soc.* **1977**, 99, 714.
- (13) George, A. L.; Hruska, F. E.; Ogilvie, K. K.; Holý, A. *Can. J. Chem.* **1978**, 56, 1170.
- (14) Schirmer, R. E.; Davies, J. P.; Noggle, J. H.; Hart, P. A. *J. Am. Chem. Soc.* **1972**, 94, 2561.
- (15) Rhodes, L. M.; Schimmel, P. R. *Biochemistry* **1971**, 10, 4426.
- (16) Hemmes, P. R.; Oppenheimer, L.; Jordan, F. *J. Am. Chem. Soc.* **1974**, 96, 6023.
- (17) Samijlenko, S. P.; Stepanyugin, A. V.; Potyahaylo, A. L.; Hovorun, D. M. *Proc. SPIE* **2004**, 5507, 358.
- (18) Samijlenko, S. P. *Dopov. Nats. Akad. Nauk Ukr. (Ukrainian)* **2003**, 7, 161.
- (19) Nir, E.; Hünig, I.; Kleinermanns, K.; de Vries, M. S. *ChemPhysChem* **2004**, 5, 131.
- (20) Ivanov, A. Yu.; Krasnokutski, S. A.; Sheina, G. G.; Blagoi, Yu. P. *Spectrochim. Acta, Part A* **2003**, 59, 1959.
- (21) Ivanov, A. Yu.; Sheina, G. G.; Krasnokutski, S. A. *Low Temp. Phys.* **2003**, 29, 809.
- (22) Shishkin, O. V.; Pelmenchikov, A.; Hovorun, D. M.; Leszczynski, J. *J. Mol. Struct.* **2000**, 526, 329.
- (23) Foloppe, N.; MacKerell, A. D., Jr. *J. Phys. Chem. B* **1998**, 102, 6669.
- (24) Foloppe, N.; MacKerell, A. D., Jr. *Biophys. J.* **1999**, 76, 3206.
- (25) Hocquet, A.; Leulliot, N.; Ghomi, M. *J. Phys. Chem. B* **2000**, 104, 4560.
- (26) Hocquet, A.; Ghomi, M. *Phys. Chem. Chem. Phys.* **2000**, 2, 5351.
- (27) Leulliot, N.; Ghomi, M.; Scalmani, G.; Berthier, G. *J. Phys. Chem. A* **1999**, 103, 8716.
- (28) Foloppe, N.; Nilsson, L.; MacKerell, A., Jr. *Biopolymers* **2002**, 61, 61.
- (29) Brameld, K. A.; Goddard, W. A. *J. Am. Chem. Soc.* **1999**, 121, 985.
- (30) Foloppe, N.; Hartmann, B.; Nilsson, L.; MacKerell, A., Jr. *Biophys. J.* **2002**, 82, 1554.
- (31) Shishkin, O. V.; Pelmenchikov, A.; Hovorun, D. M.; Leszczynski, J. *Chem. Phys.* **2000**, 260, 317.
- (32) Pelmenchikov, A.; Hovorun, D. M.; Shishkin, O. V.; Leszczynski, J. *J. Chem. Phys.* **2000**, 113, 5986.

- (33) Krokan, H. E.; Drabløs, F.; Slupphaug, G. *Oncogen* **2002**, 21, 8935.
- (34) Pearl, L. H. *Mutat. Res.* **2000**, 460, 165.
- (35) Krokan, H. E.; Nilsen, H.; Skorpen, F.; Otterlei, M.; Slupphaug, G. *FEBS Lett.* **2000**, 476, 73.
- (36) Kavli, B.; Otterlei, M.; Slupphaug, G.; Krokan, H. E. *DNA Repair* **2007**, 6, 505.
- (37) Chaundhuri, Y.; Tian, M.; Khuong, C.; Chua, K.; Pinaud, E.; Alt, F. W. *Nature* **2003**, 422, 726.
- (38) Yurenko, Ye. P.; Zhurakivsky, R. O.; Ghomi, M.; Samijlenko, S. P.; Hovorun, D. M. *J. Phys. Chem. B* **2007**, 111, 6263.
- (39) Zhurakivsky, R. O.; Yurenko, Ye. P.; Hovorun, D. M. *Dopov. Nats. Akad. Nauk Ukr. (Ukrainian)* **2006**, 8, 207.
- (40) Becke, A. P. *J. Chem. Phys.* **1993**, 98, 5648.
- (41) Parr, R. G.; Yang, W. *Density Functional Theory of Atoms and Molecules*; Oxford University Press: New York, 1989.
- (42) Lee, C.; Yang, W.; Parr, R. G. *Phys. Rev. B* **1988**, 37, 785.
- (43) Peng, C.; Schlegel, H. B. *Isr. J. Chem.* **1993**, 33, 449.
- (44) Frisch, M. J.; Trucks, G. W.; Schlegel, H. B.; Scuseria, G. E.; Robb, M. A.; Cheeseman, J. R.; Montgomery, J. A., Jr.; Vreven, T.; Kudin, K. N.; Burant, J. C.; Millam, J. M.; Iyengar, S. S.; Tomasi, J.; Barone, V.; Mennucci, B.; Cossi, M.; Scalmani, G.; Rega, N.; Petersson, G. A.; Nakatsuji, H.; Hada, M.; Ehara, M.; Toyota, K.; Fukuda, R.; Hasegawa, J.; Ishida, M.; Nakajima, T.; Honda, Y.; Kitao, O.; Nakai, H.; Klene, M.; Li, X.; Knox, J. E.; Hratchian, H. P.; Cross, J. B.; Adamo, C.; Jaramillo, J.; Gomperts, R.; Stratmann, R. E.; Yazyev, O.; Austin, A. J.; Cammi, R.; Pomelli, C.; Ochterski, J. W.; Ayala, P. Y.; Morokuma, K.; Voth, G. A.; Salvador, P.; Dannenberg, J. J.; Zakrzewski, V. G.; Dapprich, S.; Daniels, A. D.; Strain, M. C.; Farkas, O.; Malick, D. K.; Rabuck, A. D.; Raghavachari, K.; Foresman, J. B.; Ortiz, J. V.; Cui, Q.; Baboul, A. G.; Clifford, S.; Cioslowski, J.; Stefanov, B. B.; Liu, G.; Liashenko, A.; Piskorz, P.; Komaromi, I.; Martin, R. L.; Fox, D. J.; Keith, T.; Al-Laham, M. A.; Peng, C. Y.; Nanayakkara, A.; Challacombe, M.; Gill, P. M. W.; Johnson, B.; Chen, W.; Wong, M. W.; Gonzalez, C.; Pople, J. A. *Gaussian 03*; Gaussian, Inc.: Pittsburgh, PA, 2003.
- (45) Kitamura, K.; Wakahara, A.; Mizuno, H.; Baba, Y.; Tomita, K. *J. Am. Chem. Soc.* **1981**, 103, 3899.
- (46) von Schilling, H. *Statistische Physik in Beispielen*; VEB Fachbuchverlag: Leipzig, 1972.
- (47) Bader, R. F. W. *Atoms in Molecules: A Quantum Theory*; Clarendon: Oxford, 1990.
- (48) Koch, U.; Popelier, P. L. A. *J. Phys. Chem.* **1995**, 99, 9747.
- (49) Biegler-König, F. W.; Bader, R. F. W.; Tang, Y. H. *J. Comput. Chem.* **1982**, 3, 317.
- (50) Grabowski, S. J. *Chem. Phys. Lett.* **2001**, 338, 361.
- (51) Grabowski, S. J. *J. Phys. Chem. A* **2001**, 105, 10739.
- (52) Iogansen, A. V. In *Hydrogen Bond*; Nauka: Moscow, 1981; p 112 (in Russian).
- (53) Altona, C.; Sundaralingam, M. *J. Am. Chem. Soc.* **1972**, 94, 8205.
- (54) Hobza, P.; Šponer, J. *Chem. Rev.* **1999**, 99, 3247.
- (55) Yurenko, Ye. P.; Zhurakivsky, R. O.; Ghomi, M.; Samijlenko, S. P.; Hovorun, D. M. *J. Phys. Chem. B* **2007**, 111, 9655.
- (56) Berman, H. *Biopolymers* **1997**, 44, 23.
- (57) Schneider, B.; Berman, H. M. In *Computational Studies of RNA and DNA*; Šponer, J., Lankaš, F., Leszczynski, J., Eds.; Springer: New York, 2006; p 1.
- (58) Ivanov, V. I.; Minchenkova, L. E. *Mol. Biol. (Engl. Ed.)* **1995**, 28, 780.
- (59) Berti, P. J.; McCann, J. A. B. *Chem. Rev.* **2006**, 106, 508.
- (60) Kunkel, T. A.; Wilson, S. H. *Nature* **1996**, 384, 25.
- (61) Slupphaug, G.; Mol, C. D.; Kavli, B.; Arvai, A. S.; Krokan, H. E.; Tainer, J. A. *Nature* **1996**, 384, 87.
- (62) Mol, C. D.; Arvai, A. S.; Begley, T. J.; Cunningham, R. P.; Tainer, J. A. *J. Mol. Biol.* **2002**, 315, 373.
- (63) Liu, P.; Burdzy, A.; Sowers, L. C. *Chem. Res. Toxicol.* **2002**, 15, 1001.
- (64) Matta, C. F.; Castillo, N.; Boyd, R. J. *J. Phys. Chem. B* **2006**, 110, 563.
- (65) Matta, C. F.; Bader, R. F. W. *Proteins: Struct., Funct., Genet.* **2000**, 40, 310.
- (66) Herman, H.; Hertz, H. G.; Maurer, R. *Chimia* **1985**, 39, 61.
- (67) Matta, C. F. In *Hydrogen Bonding: New Insights*; Grabowski, S. J., Leszczynski, J., Eds.; Springer: New York, 2006; p 337.
- (68) Bondi, A. *J. Phys. Chem.* **1964**, 68, 441.
- (69) Hocquet, A. *Phys. Chem. Chem. Phys.* **2001**, 3, 3192.
- (70) Louit, G.; Hocquet, A.; Ghomi, M. *Phys. Chem. Chem. Phys.* **2002**, 4, 3843.